IUST
Iran University of Science and Technology

Iranian Journal of Electrical and Electronic Engineering

Journal Homepage: ijeee.iust.ac.ir

Research Paper

A Novel Implementation of SVM-DTC: Integrated Control of IPM Motor and Hybrid Energy Storage System for Electric Vehicle Application

M. Habibzadeh* and S. M. Mirimani*(C.A.)

Abstract: The role of energy management in hybrid and electric vehicles (EVs) is an important concern to enhance operational performance and provide the defined efficiency targets in transportation. The power conversion stage as an interface between storage units and the DC-link of the three-phase inverter forms a major challenge in EVs. In this study, a control approach for DC-bus voltage, which utilizes a hybrid energy storage system (HESS) for EV applications, has been proposed. A high-energy-density battery pack and an ultra-capacitor, which owns a high-power density, form the hybrid energy storage system. The proposed approach allows full utilization of the stored energy in the storage devices, and also adds a voltage boost feature to the DC-bus. In the proposed control structure, a motor drive based on SVM-DTC is used to track the flux and torque components using regulators with the space vector modulation. The optimal DC-bus voltage can be tracked by incorporating the motor drive stage with a HESS. This integration results in less processed power. This article presents the simulation results toward confirming and verifying the effectiveness of the proposed approach.

Keywords: Battery, DC/DC Converter, Electric Vehicles, Hybrid Energy Storage System (HESS), Ultra-Capacitor (UC).

1 Introduction

THE aggravating problem of global warming and the exacerbating environmental pollution push the governments and the private sectors to decrease the reliance on fossil fuels and invest in the electric vehicle (EV) area [1]. Energy storage systems in the EVs should afford long-distance driving and they must be enough to meet different performances in a car, including acceleration, braking, climbing, etc. Some battery types cover both features of high-power density and high-energy density, but overheating is very potential in these battery packs and their lifetime is short [2]. The aforementioned disadvantages made the researchers focus on integrating batteries with other storage devices to form a hybrid storage system. Ultra-capacitors own interesting features, including high-power density, high efficiency, fast charge, and wide operational range. These characteristics have made ultra-capacitors an interesting choice in energy storage systems. The hybrid energy storage system (HESS) and battery system integration is capable of utilizing all advantages of both devices. In this type of HESS, batteries are responsible for covering the average power demands, while ultra-capacitors are most useful in transient high-power delivery [3].

In this article, a bidirectional DC/DC power electronic circuitry for the HESS is proposed to drive an interior permanent magnet (IPM) motor. In order to enhance the system performance through an increase in the bus voltage in the motor flux-weakening operating region, earlier studies have suggested a variable DC bus voltage [4]. Theoretically, there are two control schemes of high-speed operation for permanent magnet synchronous machines (PMSMs). The most popular one is the field weakening control, and the other choice is the voltage control method. The field weakening control

Iranian Journal of Electrical and Electronic Engineering, 2021.
Paper first received 08 July 2020, revised 16 May 2021, and accepted 28 May 2021.
* The authors are with the Department of Electrical and Computer Engineering, Babol Noshirvani University of Technology, Babol, Iran.
E-mails: mohsen.habibzadeh74@gmail.com and mirimani@nit.ac.ir.
Corresponding Author: S. M. Mirimani.
https://doi.org/10.22068/IJEEE.17.4.1931

sets an adequate current in the d-axis to mitigate the air-gap flux linkage in order to speed up the system operation under finite DC-link voltage restriction. Hence, the magnitude of the associated current vector increases in the field weakening zone. This process leads to more copper loss in comparison with the low-speed zone. The main concept in the voltage control system is making adjustable DC-link voltage with the operation planned. Therefore, the d-axis current is no longer needed in the mid-to-high speed zone. The voltage control usually requires an additional DC-DC converter to perform boost/buck operation as the interconnecting power conversion stage between the voltage source and the inverter. This extra structure increases the system volume and cost. In addition, the switching and conducting power loss in the DC-DC converter decreases the total system efficiency [5, 6].

In this study, the flux and torque control by means of space vector modulation (SVM) was used for an IPMSM proposed in [7, 8]. Here, owing to the characteristics, including flux and torque concurrent control and less sensitivity to disturbances, the closed-loop flux and torque control on the stator flux-oriented coordinates is applied. Two PI controllers are applied, using this system, for flux and torque control at the same time. Reference voltage vector generated in the rotary setting thus makes the system comparable to the field-oriented control. The drivetrain performance may further be enhanced by choosing an effective control strategy, besides high effective IPMSM for its configuration. Since vector control methods have better dynamic control, they appear more promising. Two chief vector control methods include direct torque control (DTC) and field-oriented control (FOC) systems. DTC does not need coordinate transformation and current regulator compared to field-oriented FOC. Moreover, compared to FOC, DTC has less sensibility to the motor parameters. The merit of a closed-loop controller with PI is the ability to eradicate the steady-state error due to imprecise parameters and modeling.

The merits of the two control systems may be found in a DTC based on space vector modulation (SVM-DTC). In the present study, SVM-DTC is, therefore, chosen to control IPMSM in the EV drivetrain.

2 Motor Drive System

A motor drive system is composed of a three-phase voltage source inverter (VSI) and a motor. The DC-bus voltage is supplied by a battery or a boost converter in the EV [5]. The interior permanent magnet (IPM) machine is a common choice in electric and hybrid vehicle applications [9].

2.1 IPM Machine Model

Typically for IPM motors, the dynamic model is formulated in the rotor reference frame:

$$V_d = R_s i_d + \frac{d\Psi_d}{dt} - \omega_r \Psi_q \tag{1}$$

$$V_q = R_s i_q + \frac{d\Psi_q}{dt} - \omega_r \Psi_d \tag{2}$$

$$\Psi_d = L_d i_d + \Psi_{PM} \tag{3}$$

$$\Psi_q = L_q i_q \tag{4}$$

$$T_e = \frac{3}{2}\frac{P}{2}\left[\Psi_{PM} i_q + \left(L_d - L_q\right)\left(i_q i_d\right)\right] \tag{5}$$

Where P represents the number of poles, V is the voltage, R_s indicates the phase resistance, i is the current, and Ψ, L, and ω_r represent the flux linkage, the inductance, and the speed, respectively. Besides, d and q are associated with the standard, permanent magnet direct, and quadrature axes.

2.2 Flux and Torque Control by Means of Space Vector Modulation (SVM)

The block diagram for this control method is shown in Fig. 1. The input signals of the two PI regulators in Fig. 1 are formed by the two error signals. The error signals are the result of the subtraction of the stator flux and torque reference values from their estimated values. Finally, the reference voltage vector using SVM block is used to control the inverter. The main differences of this structure with conventional DTC are the replacement of conventional DTC hysteresis controllers with two torque and flux PI controllers as well as the

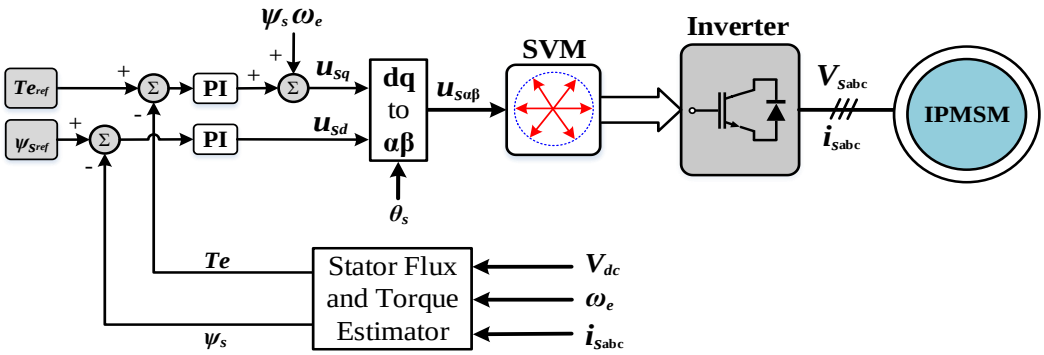

Fig. 1 Block diagram of SVM DTC control method with two PI controllers.

replacement of the switching table in the DTC by Space Vector Modulation (SVM). According to Fig. 1, the back EMF term, $\Psi_s\omega_e$ is explicitly compensated in a feedforward manner to avoid deterioration of the performance of the torque regulator, especially at high speeds. Provided that the stator flux is tightly regulated, the gains of the torque controller k_i and k_p can be selected according to classical control theory to meet the transient requirements [10].

In conventional DTC, there was a relatively high torque and flux ripple. This basic DTC problem is due to improper selection of stator voltage vector and the use of a hysteresis loop. In a three-phase inverter, the space voltage vector can be generated by eight base voltage vectors using the SVM method. The space vector of the voltage depends on the generated voltage values by the PI regulators in the applied approach. Hence, the stator flux linkage and torque can be tuned accurately, and consequently, the constant switching frequency is attained. The voltage vector should be converted to the reference frame (α–β). The magnitude of the reference voltage vector can be derived as follows:

$$\left|\bar{V}_{ref}\right| = \sqrt{V_\alpha^2 - V_\beta^2} \tag{6}$$

With the SVM technique, the space vector voltage is obtained by combining two active voltage vectors and a zero-voltage vector as shown in Fig. 2. For example, when the reference voltage $\bar{V}_{ref}$ is between voltage $\bar{V}_1$ and $\bar{V}_2$, it is expressed as follows:

$$\bar{V}_{ref} = \bar{V}_0\frac{T_0}{T_s} + \bar{V}_1\frac{T_1}{T_s} + \bar{V}_2\frac{T_2}{T_s} \tag{7}$$

Where T_0, T_1, and T_2 are respectively the time of the voltage applied by V_0, V_1, and V_2 at the sampling time T_s, which according to Fig. 3 are obtained by (8) and (9).

$$\begin{cases} V_{ref}\cos\alpha = V_1\dfrac{T_1}{T_s} + V_2\dfrac{T_2}{T_s}\cos\dfrac{\pi}{3} \\ V_{ref}\sin\alpha = V_2\dfrac{T_2}{T_s}\sin\dfrac{\pi}{3} \end{cases} \tag{8}$$

$$\begin{cases} T_1 = \dfrac{V_{ref}\sin(\frac{\pi}{3}-\alpha)}{V_1\sin\frac{\pi}{3}} \\ T_2 = \dfrac{V_{ref}\sin(\alpha)}{V_2\sin\frac{\pi}{3}} \\ T_0 = T_s - T_1 - T_2 \end{cases} \tag{9}$$

where α is the reference vector angle with the horizontal axis varying between the interval $0 \geq \alpha \geq 60°$.

The stator flux linkage estimation is performed using the motor terminal voltages (V_{sq} and V_{sd}) and the stator currents (i_{sq} and i_{sd}). The equations for stator flux estimation, stator flux vector angle, and electromagnetic torque are as follows:

$$\begin{cases} \hat{\Psi}_{sd} = \int (V_{sd} - R_s i_{sd})dt \\ \hat{\Psi}_{sq} = \int (V_{sq} - R_s i_{sq})dt \end{cases} \tag{10}$$

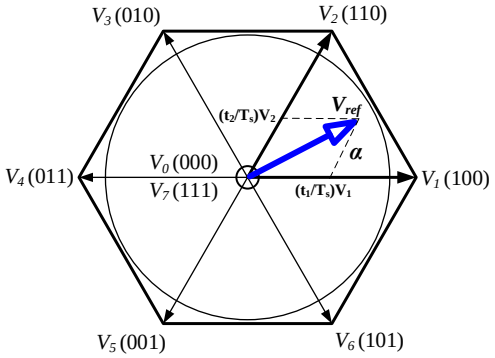

Fig. 2 Types of replication schemes.

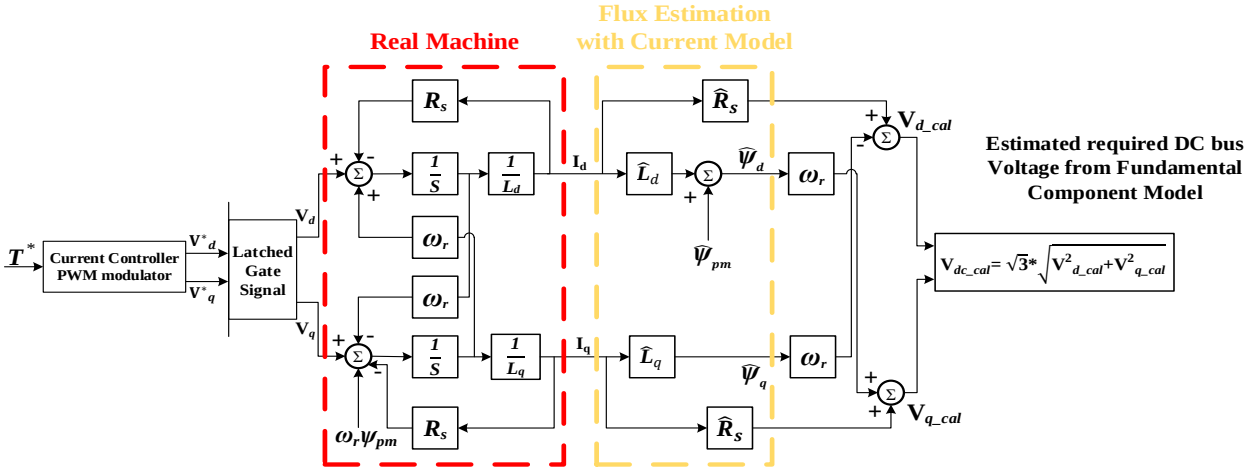

Fig. 3 Block diagram of SVM DTC control method with two PI controllers.

$$\hat{\theta}_s = \tan^{-1}\left(\frac{\hat{\Psi}_{sq}}{\hat{\Psi}_{sd}}\right) \quad (11)$$

$$\hat{T_e} = \frac{3}{2}.\frac{P}{2}\left[\hat{\Psi}_{sd} i_{sq} - \hat{\Psi}_{sq} i_{sd}\right] \quad (12)$$

The DC bus voltage is calculated using the fundamental component method proposed in [4] and [6], that is:

$$V_{dc\_cal} = \sqrt{3} \times \sqrt{\left(\omega_r L_q i_q\right)^2 + \left(\omega_r L_d i_d + \Psi_{PM}\right)^2} \quad (13)$$

As demonstrated in Fig. 3, V_{dc_cal} is calculated using the fundamental component (FC) technique.

3 Principle and Configuration of the Integrated System

The topology architecture and energy management control technique form two dominant features of a hybrid system. Fig. 4 shows four common topology structures, which can be categorized into three types: passive, semi-active, and fully active. The passive topology, which is depicted in Fig. 4(a), possesses the simplest architecture, and no control scheme has been applied to this topology. Lack of control in the DC-side of the system is the main disadvantage of this structure. However, a proper control algorithm is needed to make the most of the ultra-capacitor in the system. As demonstrated in Fig. 4(b), the semi-active topology is composed of a DC-DC converter, an ultra-capacitor, and a battery. Unlike passive topology, the power exchange process is controlled by monitoring the voltage and sensing the supplied current. The main drawback of this structure is the wide oscillation of the voltage across the DC-bus, which may cause a bad impact on the motor supply. The main drawback of this structure is the wide oscillation of the voltage across the DC-bus, which may cause a bad impact on the motor supply. Fig. 4(c) shows a different kind of semi-active topology. In this topology, the DC-DC converter interconnects the ultra-capacitor and the battery/DC-bus. Therefore, with the help of the interfacing DC-DC converter, the voltage of the ultra-capacitor can be controlled to increase the efficiency of the power distribution. Fig. 4(d) depicts the fully active topology. In this structure, the battery and the ultra-capacitor are controlled separately, which leads to more accuracy in the control performance of the system. Semi-active topology is the best choice as a trade-off between control performance and system cost in EV applications [11, 12].

3.1 Circuit Structure and Operating Principles of the HESS Concept

Different HESS configurations have been investigated to incorporate the battery pack and the ultra-capacitor in the electric vehicle system. The applied hybrid energy storage design has been presented in [11]. The applied HESS topology increases the efficiency of the ultracapacitor while reducing the power stress on interconnecting DC-DC converter. Besides, the voltage of the DC-bus has been regulated for different operation modes.

Fig. 5 depicts different operation modes of the HESS, and the respective circuit configuration. As shown in Fig. 5, the bypass diode (D_b), which is in parallel with the converter and ultra-capacitor set, provides a bypass

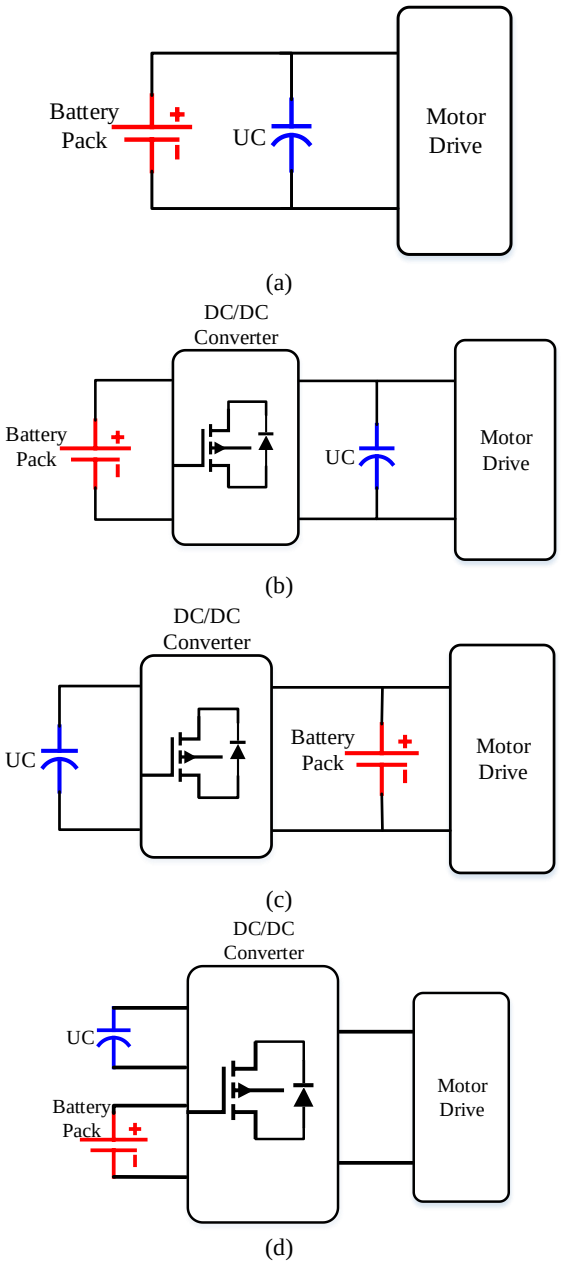

Fig. 4 Common topologies in hybrid energy storage systems: a) A passive topology structure, b) A semi-active topology, in which DC-DC converter interconnects battery with ultra-capacitor/DC-bus, c) A semi-active topology, in which DC-DC converter interconnects the ultra-capacitor and the battery/DC-bus, and d) A fully active topology structure.

over the DC-DC converter. When the voltage level is low, the bypass diode (D_b) operates and the battery feeds the DC-bus directly. The bidirectional DC-DC converter is responsible for DC-bus voltage regulation and it arranges the power-sharing among the storage devices. In acceleration intervals where high voltage is required, mode Ⅰ is activated. The ultra-capacitor and the DC-DC converter, which is fed by the battery, supply power for the DC-bus in this mode. The MOSFET (M_1) and the respective reverse-parallel diode (D_1) are the elements of the circuit configuration that operate to enable the buck converter in acceleration mode. Hence, in this mode, it is assumed that the following inequality is governing:

$$V_{UC} \geq V_{UCL} \tag{14}$$

where V_{UC} represents the voltage of the ultra-capacitor and V_{UCL} is the allowed lower limit for the ultra-capacitor. The less V_{UCL} gets, the more the capacity usage of the ultra-capacitor increases. When the ultra-capacitor fully discharges or a braking interval initiates, mode Ⅰ comes to an end. According to the following equations, the power is shared among the battery and the ultra-capacitor.

$$P_B = P_C = V_B I_B = (V_{DC} - V_{UC}) I_{DC} \tag{15}$$

$$P_{UC} = V_{UC} I_{DC} \tag{16}$$

$$P_T = P_B + P_{UC} \tag{17}$$

$$\frac{P_C}{P_T} = 1 - \frac{V_{UC}}{V_{DC}} \tag{18}$$

where P_B represents the battery power, V_B is the voltage, and I_B indicates the current. The DC-bus voltage and current are represented in the above equations as V_{DC} and I_{DC}, respectively. Additionally, P_T is the total demanded power by the electric vehicle, and P_C is associated with the processed power.

According to (18), by the reduction in the ultra-capacitor voltage, the converter processed power rises. After supplying the peak power, and when the voltage of the ultra-capacitor drops, this feature suits the EV applications.

When a low-voltage demand is required for the drive system, mode II occurs. As depicted in Fig. 5(b), in this mode, the voltage across the bypass diode is more than the threshold voltage of D_b. Therefore, D_b is enabled and conducts the power in a bypass making the battery the only supplier of the DC-bus. Bypassing the converter increases the system efficiency. In constant speed mode, the power demand of the motor is low. Therefore, fewer oscillations of DC-bus voltage have resulted. The discharging current of the battery is also decreased. As demonstrated in Fig. 5(c), the interior permanent magnet motor charges both the ultra-capacitor and the battery in the regenerative braking mode. Thanks to the DC-DC converter control unit, the supplied power by the IPM machine is shared between the battery and the ultra-capacitor. In this mode, the MOSFET (M_2) and the body diode (D_2) are being switched to provide the boost operation mode of the DC-DC converter and to regulate the DC-bus voltage. When the EV stops braking, the regenerative mode ends [11].

3.2 Proposed Control Approach

In this study, a control approach using a bidirectional DC-DC converter has been proposed to control the DC-bus voltage according to the optimal design requirements. As demonstrated in Fig. 6, the DC-DC converter is a multi-objective converter that can also be used for power-sharing between the storage devices. Based on the relationships presented, an SVM-DTC based control system with two separate PI controllers is used. The PI compensators used for regulating the flux

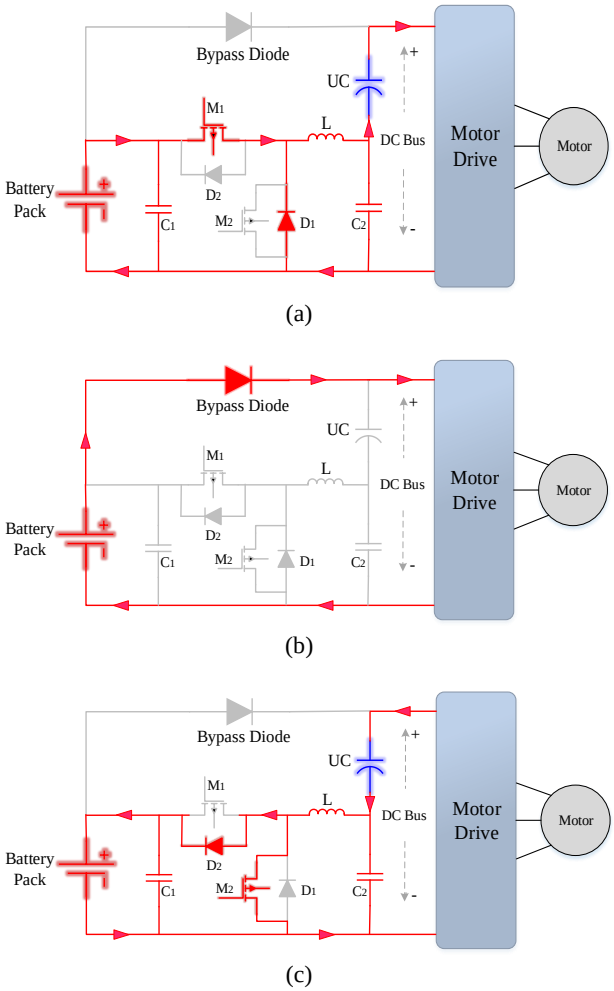

Fig. 5 Power flow in different operation modes: a) Acceleration mode–The path and the direction of the power flow in acceleration mode (Mode I), b) Constant speed mode–The path and the direction of the power flow in constant speed mode (Mode II), and c) Regenerative braking mode–The path and the direction of the power flow in regenerative mode (Mode III).

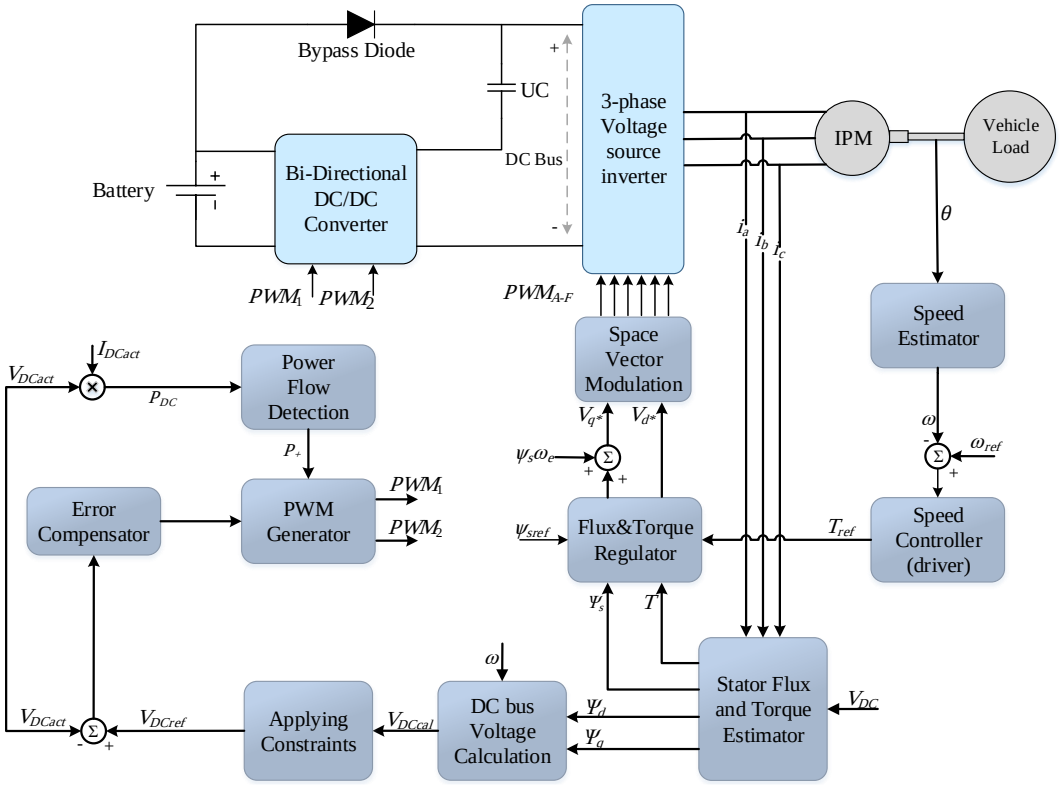

Fig. 6 Block diagram of integrated hybrid energy storage system and motor control scheme.

and the torque together with the SVM technique are responsible for controlling the flux and the torque. The voltage of the DC-bus is derived by (13), and then it can be applied as the reference voltage for the DC-bus voltage to generate the pulse width modulation signals.

Where V_{dc} and I_{dc} represent the total DC-bus voltage and current, respectively in the block diagram of Fig. 6. Additionally, the reference voltage for the DC-bus is indicated as V_{DCref}, and P_{DC} is the total motoring or regenerating power of the electric vehicle. The direction of the power flow is referred to P_+, which is a digital signal. The outputs of PWM_1 and PWM_2 in the control block diagram (Fig. 6) generate the switching signals for M_1 and M_2.

4 Simulation Results

A 50-kW three-phase interior permanent magnet machine has been considered as the case study in this paper. The investigated machine is the same as the one applied in Toyota Prius and acts as the benchmark in many studies in EV machine applications. The characteristics of the motor are summarized in Table 1. The battery pack is made up of a 550 V Li-Ion cell-pack and a 500 Volts- rating 8 F ultra-capacitor.

The system is simulated by MATLAB software for traction applications. Figs. 7, 8, and 9 demonstrate the simulation results. These results are performed under constant speed and torque conditions as well as variable speed and torque. Fig. 7 shows the response of speed, torque, motor power, UC power, and battery power

Table 1 Key parameters of the motor.

Parameters	Values
Power	50 [kW]
Torque	400 [N.m]
Speed	1200 [r/min]
DC side voltage	500 [V]
Frequency	80 [Hz]
Number of poles	8
Number of slots	48
Flux linkage (Ψ_{PM})	0.366 [Vs/rad]
q-axis inductance	8.89 [mH]
d-axis inductance	4.11 [mH]
Stator resistance	0.295 [Ω]
Highest efficiency	95%

under 1200 r/min and rated load (400 N.m).

Fig. 7 shows the system efficiency in better dynamic control. As seen, in the rated load mode, the motor speed reaches the specified rate in its reference (1200 rpm), suggesting that one of the essential factors for the motor right operation, i.e., speed stability, can be provided by the proposed electric drive system. After a transient state, the torque touches its reference rate, i.e., the motor's rated load, and varies around with a minor ripple. Three-phase currents are sinusoidal with 100 Hz frequency, as shown in Figs. 7(c)-(d). Further, these currents exhibit a difference of approximately 120 degrees.

As demonstrated in Fig. 7, the ultra-capacitor supplies

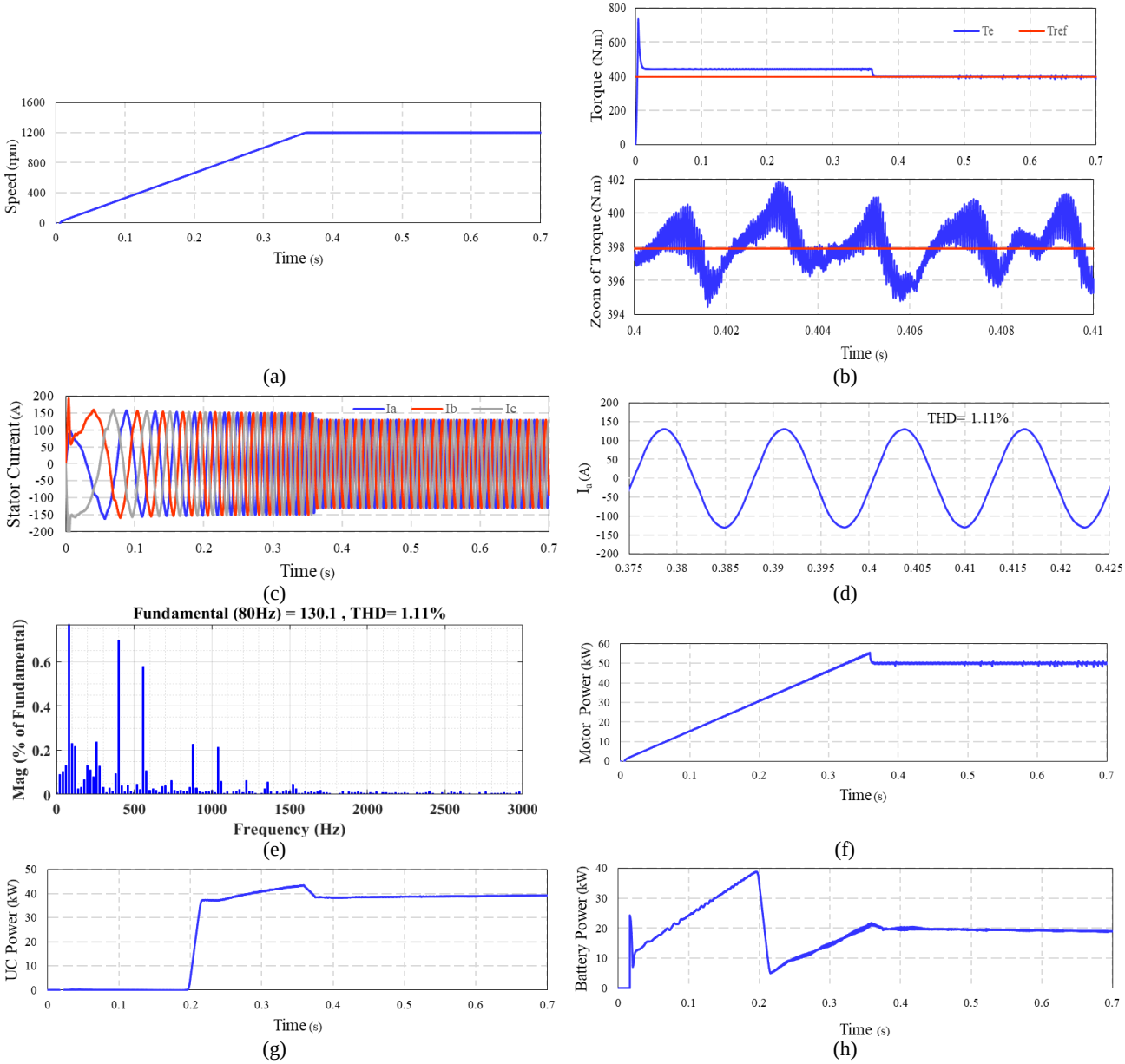

Fig. 7 Simulation results using the proposed integrated control under constant speed and torque conditions: a) Motor speed in r/min, b) Motor torque, c) Phase current of the stator, d) Phase current A of the stator, e) Stator current FFT analysis, f) Motor power, g) UC power, and h) Battery power.

most of the peak power. However, the battery provides only the average power for the motor. In the applied structure, the DC-DC converter is only fed by the battery. Nevertheless, the ultra-capacitor is responsible for the majority of the discharged EV power due to its relatively direct touch with the motor. While the DC-DC converter only provides a portion of the system power, it fully controls the total system power flow. Hence, this control approach has enhanced the efficiency of the system while decreasing the system cost.

To confirm the validity of the proposed method and to verify the results of its simulation, this method was simulated with a control system using FOC drive, and compared with the presented results. Fig. 8 shows the torque waveform and phase current A of the stator for the FOC control method.

As expected, the ripple torque in the SVM-DTC control method is larger than in the FOC control method, which is due to the nature of the DTC method.

In order to investigate the capability of the control system, the torque reference oscillates as a pulse train between two values of 100 and -50. In this way, the machine is able to operate in both motor and generator modes. Also, in this simulation, the reference speed as a pulse train from the beginning to the moment of 0.55 seconds, equal to 3600 rpm, and from the moment of 0.55 seconds to one second, the reference speed is

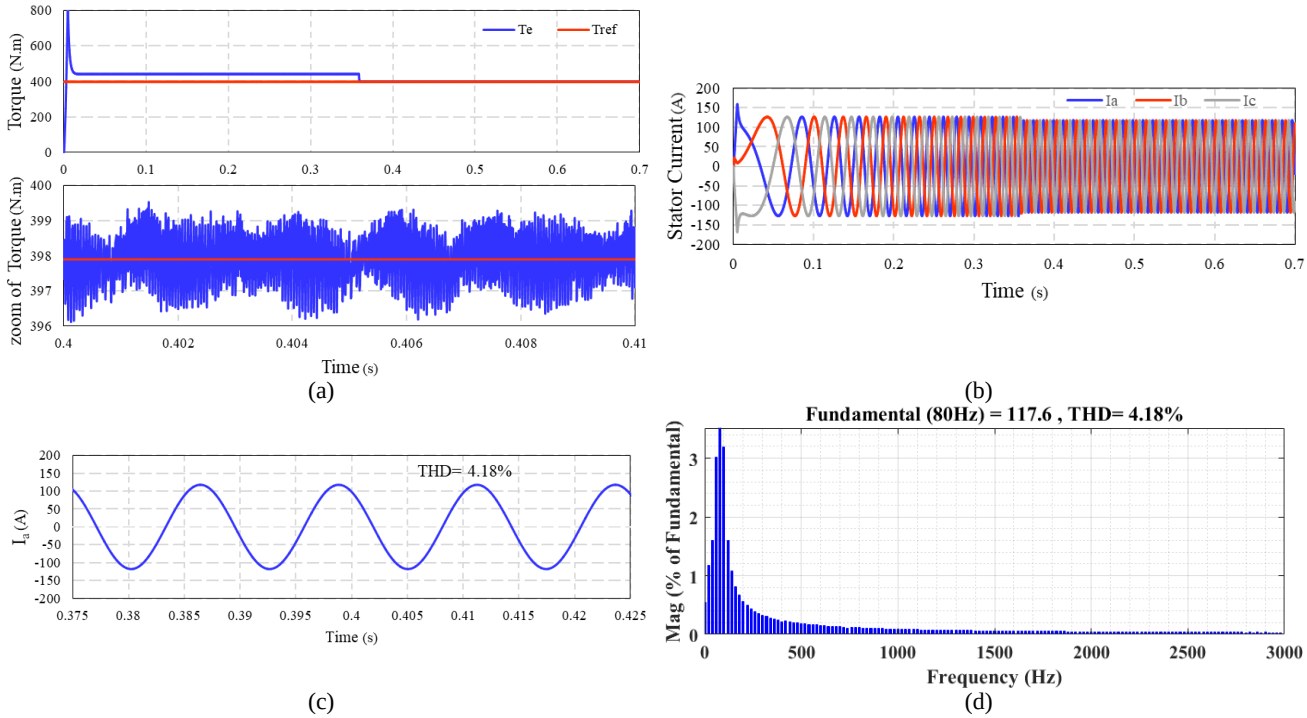

Fig. 8 Simulation results of torque and phase current A of FOC control method: a) Motor torque in N.m, b) Phase current of the stator, c) Phase current A of the stator, and d) Stator current FFT analysis.

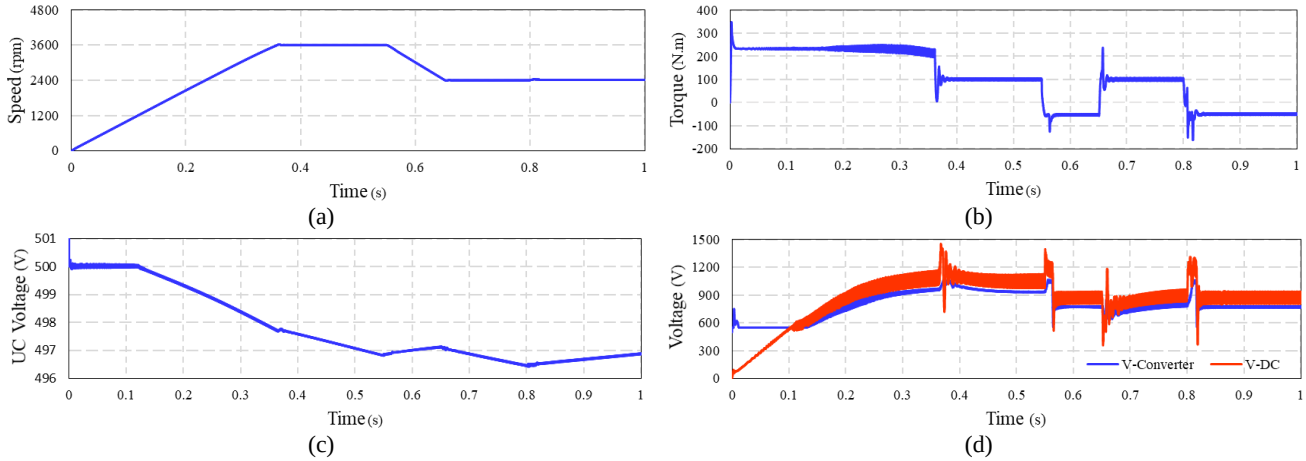

Fig. 9 Simulation results under variable speed and torque conditions: a) Motor speed in r/min, b) Motor torque in N.m, c) UC voltage, and d) Applicable DC bus and converter voltage.

reduced to 2400 rpm.

As can be seen in Fig. 9, the machine operates in motor mode from zero to 0.8 seconds. Also, with a negative torque at the moment of 0.8 seconds, the machine goes out of motor mode and enters the generator area. It can be deducted from the simulation results that by applying this circuit structure in the DC side the voltage of the DC-bus can be elevated to fulfill the load requirements. As the converter voltage increases, more current provides the DC link, so the UC voltage is discharged more rapidly.

5 Conclusion

In this study, a control approach based on space-vector-modulation direct-torque-control (SVM-DTC) motor drive controller integrated with a hybrid energy storage system (HESS) has been proposed. The proposed approach, aiming at tracking the DC-bus voltage, reduces system cost, and power loss. The output of the DC-DC converter is in series with the ultra-capacitor. This circuit configuration allows only a portion of the total system power to be transferred through the converter. Hence, the share of the processed power by the converter is decreased and this leads to less power loss and more efficiency of the system. Besides, the control of the power flow in the system is assigned to the DC-DC converter as the control unit of the HESS. The DC-DC converter can boost the DC-bus voltage whenever the load requires in special operation

modes. The simulation of the system is carried out in MATLAB/Simulink environment. Two operation scenarios are simulated to investigate the control performance. Also, the simulation results have been compared with the performance of the field-oriented-control (FOC) method. The comparisons justify the superiority of the proposed method.

References

[1] S. S. Raghavan and A. Khaligh, "Electrification potential factor: Energy-based value proposition analysis of plug-in hybrid electric vehicles," *IEEE Transactions on Vehicular Technology*, Vol. 61, No. 3, pp. 1052–1059, 2011.

[2] R. Xiong, Y. Zhang, H. He, X. Zhou, and M. G. Pecht, "A double-scale, particle-filtering, energy state prediction algorithm for lithium-ion batteries," *IEEE Transactions on Industrial Electronics*, Vol. 65, No. 2, pp. 1526–1538, 2017.

[3] L. Zhang, X. Hu, Z. Wang, F. Sun, J. Deng, and D. G. Dorrell, "Multiobjective optimal sizing of hybrid energy storage system for electric vehicles," *IEEE Transactions on Vehicular Technology*, Vol. 67, No. 2, pp. 1027–1035, 2017.

[4] C. Y. Yu, J. Tamura, and R. D. Lorenz, "Optimum DC bus voltage analysis and calculation method for inverters/motors with variable DC bus voltage," *IEEE Transactions on Industry Applications*, Vol. 49, No. 6, pp. 2619–2627, 2013.

[5] S.-M. Sue, J. H. Liaw, Y. S. Huang, and Y. H. Liao, "Design and implementation of a dynamic voltage boosting drive for permanent magnet synchronous motors," in *IEEE International Power Electronics Conference-ECCE ASIA*, pp. 1398–1402, 2010.

[6] K. Yamamoto, K. Shinohara, and T. Nagahama, "Characteristics of permanent-magnet synchronous motor driven by PWM inverter with voltage booster," IE*EE Transactions on Industry Applications*, Vol. 40, No. 4, pp. 1145–1152, 2004.

[7] K. K. Prabhakar, C. U. Reddy, P. Kumar, A. K. Singh, and S. T. I. P. Electronics, "A new reference flux linkage selection technique for efficiency improvement of direct torque controlled IM drive," *IEEE Journal of Emerging and Selected Topics in Power Electronics*, Vol. 8, No. 4, pp. 3751–3762, 2020.

[8] X. Wang, Z. Wang, and Z. Xu, "A hybrid direct torque control scheme for dual three-phase PMSM drives with improved operation performance," *IEEE Transactions on Power Electronics*, Vol. 34, No. 2, pp. 1622–1634, 2018.

[9] M. Takeno, S. Ogasawara, A. Chiba, M. Takemoto, and N. Hoshi, "Power and efficiency measurements and design improvement of a 50kW switched reluctance motor for hybrid electric vehicles," in *IEEE Energy Conversion Congress and Exposition*, pp. 1495–1501, 2011.

[10] G. H. B. Foo, T. Ngo, X. Zhang, and M. F. Rahman, "SVM direct torque and flux control of three-level simplified neutral point clamped inverter fed interior PM synchronous motor drives," *IEEE/ASME Transactions on Mechatronics*, Vol. 24, No. 3, pp. 1376–1385, 2019.

[11] M. O. Badawy and Y. Sozer, "A partial power processing of battery/ultra-Capacitor hybrid energy storage system for electric vehicles," in *IEEE Applied Power Electronics Conference and Exposition (APEC)*, pp. 3162–3168, 2015.

[12] Q. Zhang and G. Li, "Experimental study on a semi-active battery-supercapacitor hybrid energy storage system for electric vehicle application," *IEEE Transactions on Power Electronics*, Vol. 35, No. 1, pp. 1014–1021, 2019.

M. Habibzadeh was born in Tehran, Iran, in 1995. He received the B.Sc. degree in Electrical Engineering from Sadra Institute of Higher Education, Tehran, Iran, in 2017, the M.Sc. degree in Electrical Engineering from Babol Noshirvani University of Technology, Babol, Iran in 2020. His current research interests include power electronic and design, renewable energy, simulation, modeling and control of electrical machines.

S. M. Mirimani was born in Babol, Iran. He received the B.Sc. degree from the University of Mazandaran, Babol, in 2007 and the M.Sc. and Ph.D. degrees on the subject of Electrical Machines from Iran University of Science and Technology, Tehran, Iran, in 2013. He is currently an Assistant Professor of Electrical Machines in Babol (Noshirvani) University of Technology, Iran. His research interests include the design, modeling, control, and finite-element analysis of electrical machines and other electromagnetic devices.

© 2021 by the authors. Licensee IUST, Tehran, Iran. This article is an open access article distributed under the terms and conditions of the Creative Commons Attribution-NonCommercial 4.0 International (CC BY-NC 4.0) license (https://creativecommons.org/licenses/by-nc/4.0/).